

THEORY OF UNDULATORS AND WIGGLERS

P. Elleaume

ESRF, Grenoble, France

38043 Grenoble Cedex, France

ABSTRACT

This paper summarises the theory of undulators and wigglers emphasis being placed on the use of wigglers for machine control and as a source of synchrotron radiation. The algebra which constitutes the basis of any numerical simulation of undulators or wiggler radiation is presented.

1. INTRODUCTION

Spatially periodic arrays of magnets were already installed and tested on linear accelerators as early as 1953 [1], this effort receiving a new start in 1976 by the first observation of amplified radiation on a superconducting helical undulator [2] installed in the superconducting linear accelerator at Stanford. For storage rings, the first such device was the Robinson wiggler [3] which was not proposed for generating radiation but as a means to improve the control of the size of the beams stored in the ring. In the late 1970s, the very first insertion of undulators on circular accelerators were performed almost simultaneously in Europe (LURE), USA (SSRL) and USSR (Lebedev, Tomsk, Novosibirsk). The purpose was to enhance the synchrotron radiation flux over that from a normal bending magnet. Nowadays, every laboratory has tested one or several of these insertion devices (ID's). The power generated has gradually increased and a few devices have reached the multikilowatt regime. Under the pressure from both synchrotron radiation users and Free Electron Laser developers, the technology of the ID has now reached some maturity. Various unconventional or 'exotic' ID's have been proposed and tested. To take full advantage of them, new machines are being optimized for a very low emittance with a large number of long straight sections. The first of these machines, the so-called third generation, is SuperACO which has recently started operation in the VUV wavelength. From a 64m total perimeter, as many as six ID's 2 to 3m long will be installed. New machines designed to operate around 1.5 GeV are being built to generate brilliant beams of radiation in the soft X-ray domain such as the ALS at Berkeley, the SRRC in Taiwan, ELETTRA in Trieste, and BESSY II in Berlin. Larger facilities are foreseen to cover the hard X-ray domain with undulator radiation and machines running at 6 to 8 GeV. Such projects exist in Europe (ESRF in Grenoble) in the USA (APS at Argonne) and in Japan (Riken). The ESRF, for which construction has just started, will have 29 straight sections each 5m long and available for all kind of ID's optimized for each experiment.

2. GENERALITIES

The principle of an ID is to enhance the synchrotron radiation emission as much as possible without perturbing the stored beam. The particles in the beam can be electrons (easiest and cheapest) or positrons (for a better lifetime and stability). The radiation properties of both kinds of particles are indistinguishable, and in the following I shall only refer to electrons because they are the most widely used. Insertion devices are magnetic units like the dipoles, quadrupoles, sextupoles, etc. constituting the storage ring or the accelerator in which they are mounted. Unlike the latter, however they are a non-essential part of the accelerator and can be installed, removed or replaced in a very short time. Ideally they are as decoupled as possible from the electron optics of the accelerator. One of the main requirements is, therefore, that an electron does not suffer any net deviation or angle when crossing an ID. Moreover, one typically wants to accumulate radiation along a preferred direction inside a beam line. Small angles of the trajectory are therefore desirable all along the device. For these reasons, the field is periodic and its integral along s (the main direction of propagation of the electron, see Fig. 1) must be zero.

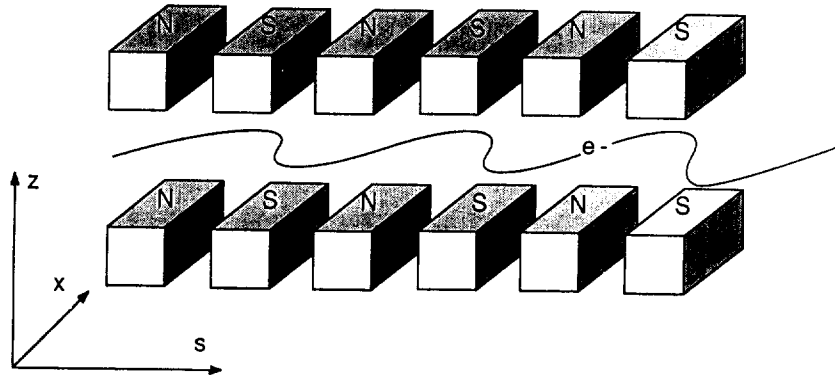


Fig. 1 Schematic of an undulator

The most conventional undulator presents a planar sinusoidal field:

$$B_z(s) = B_1 \cos(2\pi s / \lambda_0) \quad (2-1)$$

This is usually generated by an array of permanent magnets which must be as close as possible to the electrons in order to be efficient but not so close that they reduce the lifetime of the stored beam. The injection requirements, the general tendency of the closed orbit error to be larger in the horizontal plane than the vertical one, and the natural lower vertical emittance of the beam (compared to horizontal), have for consequence that smaller magnetic gaps are possible in the vertical plane. It is therefore easier to achieve a small period with a vertical field. The sinusoidal dependence of the field is not required a priori, but results from fundamental limitations. The most general periodic field is a Fourier sum of components with amplitude B_n and period λ_0/n . The B_n component typically scales as :

$$B_n = B_0 \exp(-n\pi g/\lambda_0) \quad (2-2)$$

where g is the magnetic gap and B_0 is a constant independent of g . Clearly, harmonics of the fundamental are expected to be negligible for a small gap/period ratio (the most usual case).

The field described by Eq. (2-1) is not realistic since it does not satisfy the Maxwell equations. Better analytical expressions exist for the three components B_x , B_z , and B_s but which approximate to Eq. (2-1) on the axis of the undulator while fully satisfying the Maxwell equations. In most cases Eq. (2-1) is sufficient for deriving the essential radiation properties.

From now on I shall restrict the discussion to the planar, purely sinusoidal ID (Fig. 1) whose field is given by Eq. (2-1). For the reason discussed above, it is the easiest to build and is therefore the most commonly used. Thus, the trajectory of an electron is purely horizontal, its transverse velocity v_x and its position x are both sinusoidal and are given by :

$$v_x/c = K/\gamma \sin(2\pi s / \lambda_0) \quad (2-3)$$

$$x = \lambda_0/2\pi K/\gamma \cos(2\pi s / \lambda_0) \quad (2-4)$$

with

$$\gamma = 1957 E[\text{GeV}] \quad (2-5)$$

where c is the velocity of light and γ the electron energy divided by its rest mass energy. K is an important dimensionless factor (also called deflection parameter) given by :

$$K = 0.934 B_1[\text{Tesla}] \lambda_0 [\text{cm}] \quad (2-6)$$

It is clearly seen from Eq. (2-3) that K is the ratio between the peak angular deviation and $1/\gamma$ which is the typical aperture of the radiation cone. Therefore, as we shall see below, the spectral characteristics of the radiation from an ID strongly depend on K .

Note that the amplitude of the sinusoidal trajectory is rather small. From Eq. (2-4) one can easily deduce that the amplitude is $1.3\mu\text{m}$ for an undulator with $K = 2$, a period of 5 cm and an electron energy of 6 GeV. The largest amplitudes of motion achieved in existing ID's are in the region of a millimeter, and are obtained in very high-field, long-period devices injected with low energy electrons.

Conventional ID's are usually classified as undulators, wigglers or wavelength shifters. The classification is based essentially on the value of K which determines the properties of the radiation (see below). Roughly speaking :

- The undulator has a low K value ($K < 3$) and a large number of periods.
- The wiggler has a large K value ($K > 3$) and lower number of periods.
- The wavelength shifter has a single or a few periods but the highest field (implying a very high K value) in order to shift the spectrum toward harder X-rays.

The $K = 3$ separation is an arbitrary limit. Some authors use a different value. Another category called 'wunder' is sometimes used for intermediate devices which behave partly as wigglers and partly as undulators. The interest in making the distinction between them results from the radical difference in their angular and spectral characteristics as discussed in the next section.

3. WIGGLERS FOR MACHINE CONTROL

A storage ring is controlled essentially by adjusting a few power supplies: one large dipole supply, a limited number of medium size quadrupole and sextupole supplies, and a large number of dipole correctors (sometime also quadrupole correctors). The linear and nonlinear beam dynamics are quite sensitive to the resulting field changes. Wigglers are sometimes used to control emittance, bunch length, energy spread and spin polarization. Their effect can be quantitatively studied through the synchrotron radiation integrals [4] which for a perfectly planar machine are:

$$I_1 = \int_0^{2\pi R} \eta(s) G(s) ds \quad (3-1)$$

$$I_2 = \int_0^{2\pi R} G(s)^2 ds \quad (3-2)$$

$$I_3 = \int_0^{2\pi R} |G(s)|^3 ds \quad (3-3)$$

$$I_{3a} = \int_0^{2\pi R} G(s)^3 ds \quad (3-4)$$

$$I_4 = \int_0^{2\pi R} [1-2n(s)] \eta(s) G(s)^3 ds \quad (3-5)$$

$$I_5 = \int_0^{2\pi R} |G(s)|^3 H(s) ds \quad (3-6)$$

with

$$H(s) = \frac{1}{\beta} \left\{ \eta^2 + \left\langle \beta \eta' \frac{1}{2} \beta' \eta \right\rangle^2 \right\} \quad (3-7)$$

$$n(s) = \frac{1}{G^2} \frac{dG}{dx} \quad (3-8)$$

and the notation of M. Sands [5]. $2\pi R$ is the perimeter of the machine, x the horizontal transverse coordinate, $G(s)$ the inverse of the radius of curvature of the trajectory at the longitudinal position s , $\eta(s)$ the dispersive or off-energy function and $\eta'(s)$ its derivative with respect to s , $\beta(s)$ the betatron function and $\beta'(s)$ its derivative with respect to s .

Various performance parameters of a storage ring can be expressed in terms of these integrals. For example:

- The dilatation factor or momentum compaction α is :

$$\alpha = \frac{I_1}{2\pi R} \quad (3-9)$$

- The energy loss U_0 in one revolution in the machine due to synchrotron radiation is :

$$U_0 = \left[\frac{2}{3} r_e \frac{E^4}{(mc^2)^3} \right] I_2 \quad (3-10)$$

where E is the nominal energy of the stored electrons, r_e is the classical electron radius, and mc^2 the electron rest energy. The damping of radial betatron and energy oscillations (also called synchrotron oscillations) is proportional to the so-called damping partition factors J_x , J_z and J_ϵ :

$$J_x = 1 - \frac{I_4}{I_2} \quad (3-11)$$

$$J_z = 1 \quad (3-12)$$

$$J_\epsilon = 2 + \frac{I_4}{I_2} \quad (3-13)$$

The stationary state resulting from the excitation of both transverse and longitudinal oscillations through the quantum emission of synchrotron radiation, and their damping which also originates from the synchrotron radiation, results in a 6-dimensional Gaussian distribution of the electron population in the phase space $(x, x', z, z', s, \epsilon)$. The RMS relative energy spread is written as :

$$\left(\frac{\sigma_\epsilon}{E} \right)^2 = A \frac{I_3}{2 I_2 + I_4} \quad (3-14)$$

The horizontal beam size is

$$\frac{\sigma_{x\beta(s)}^2}{\beta(s)} = \left[A \frac{I_5}{I_2 - I_4} \beta + \eta^2 \left(\frac{\sigma_\epsilon}{E} \right)^2 \right] \quad (3-15)$$

with

$$A = \frac{55}{32 \sqrt{3}} \frac{\hbar}{mc} \left(\frac{E}{mc^2} \right)^2 \quad (3-16)$$

The electron spin precesses around the local magnetic field. The emission of a quantum of light flips the spin from the up to the down states. However the probability of up-down flipping is slightly different than the down-up one so that a net non-zero spin polarization of the electron population results. As for any spin-1/2 particles, the polarization density matrix is specified completely by a three component real vector :

$$\vec{P} = P \hat{P} = \left[\frac{(N_{up} - N_{down})}{N_0} \right] \hat{P} \quad (3-17)$$

where P is the polarization rate, N_{up} (N_{down}) denotes the number of electrons with spin up (down) along the direction \hat{P} , and $N_0 = N_{up} + N_{down}$ is the total number of electrons. The equilibrium polarization rate P_0 is (6) :

$$P_0 = \frac{8}{5 \sqrt{3}} \frac{I_{3a}}{I_3} \quad (3-18)$$

The spin polarization approaches the equilibrium value P_0 with a polarization time constant τ_p :

$$\frac{1}{\tau_p} = \frac{5 \sqrt{3}}{8} \frac{\hbar r_e}{m} \left(\frac{E_0}{mc^2} \right)^5 \frac{I_3}{2 \pi R} \quad (3-19)$$

While the polarization of an initially unpolarized beam evolves as $P_0 \left[1 - \exp\left(-\frac{t}{\tau_p}\right) \right]$.

All six integrals strongly depend on the local magnetic field which is proportional to G . It turns out that even though no net deviation can be expected from an ID, its field modifies all six integrals, resulting in a modification of the equilibrium electron beam sizes, angular spreads, bunch length, energy spread and spin polarisation. The effect is usually weak. However, high field wigglers are sometimes installed on purpose in order to modify selectively one or a few of these integrals.

Robinson wigglers [3, 7] were the first to be proposed. They are essentially made of alternating poles with opposite gradients and placed in a dispersive section of non-zero η in such a way that their contribution to I_4 is negative. A net increase (decrease) of the damping partition number J_x (J_e) results together with a decrease (increase) of the emittance (bunch length and energy spread). Such a wiggler also modifies the other integrals.

Conventional wigglers have also been proposed to be placed in sections with no dispersion ($\eta = 0$). They do not contribute to I_1 , I_4 and I_5 but only to I_2 , I_3 and I_{3a} . A lower emittance results at the price of a higher energy loss per turn.

The case of LEP is of special interest in this respect. The requirement of minimizing RF power implies a low field in the bending magnet and therefore a large diameter of the machine. High field wigglers installed in LEP are therefore quite efficient for modifying the integrals in which a high exponent of $G(s)$ takes place, namely I_3 to I_5 . They offer a simple means to efficiently control emittance, bunch length and energy spread [8]. Such wigglers also have the advantage of considerably shortening the polarization time (through I_3). However, conventional wigglers lower the optimum polarization rate from 0.92 to 0.74. For colliding beam experiments which require spin polarization, assymetric wigglers have been studied in order to restore a 0.88 spin polarization. Such assymetric wigglers have different positive and negative fields while maintaining the overall field integral at zero.

All wigglers which have been used so far for machine control were electro-magnets. They present a rather long spatial period and a high field.

4. UNDULATORS AND WIGGLERS FOR SYNCHROTRON SOURCES

Synchrotron radiation is typically emitted in a cone whose angle is $1/\gamma$. Since the maximum horizontal angle of the electrons while crossing the undulator is K/γ (Eq. (2-3)), one realizes that if $K < 1$, an observer located on the axis of such an undulator sees the radiation emitted all along the undulator. On the other hand, if $K \gg 1$ the observer only sees the electrons twice per period when their velocity is directed towards him. The observed spectrum of the radiation is drastically different in the two extreme cases.

If $K \gg 1$ (wiggler case) the spectrum looks very much like the one generated by a bending magnet. The critical energy is :

$$E_c = 0.665 E^2 [\text{GeV}] B [\text{T}] \quad (4-1)$$

where E is the electron energy and B the peak undulator field. In most cases, the radiation emitted by each point does not interfere and the flux observed is simply equal to $2N$ that of a bending magnet whose field is B . The critical energy can be seen as a median energy which splits the power spectrum into two parts of equal power. Figure 2 presents the spectral flux of photons per unit horizontal angle generated by a 20 - pole wiggler of 1.5 Tesla field. The electron energy is 6 GeV and the stored current 100 mA.

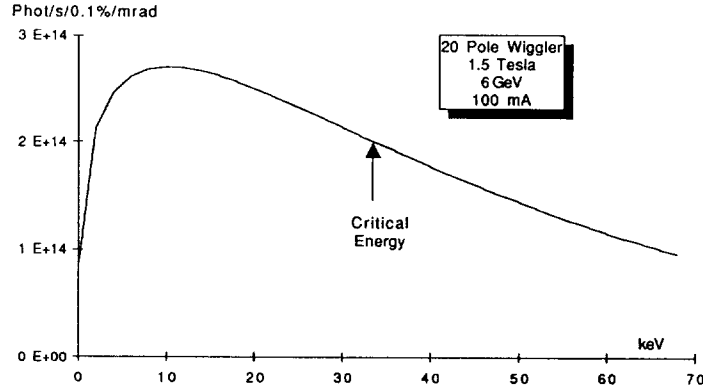


Fig. 2 Flux from a Wiggler installed at the ESRF

The large horizontal angular extension ($2K/\gamma$) of the electron motion results in a wide horizontal aperture of the radiation beam allowing a single wiggler to be shared among various experimental stations. In a direction of observation making an angle θ with the wiggler axis, the critical energy is roughly given by :

$$E_c[\theta] = E_c[\theta=0] \sqrt{1 - \frac{\theta \gamma}{K}} \quad (4-2)$$

If $K < 1$ the emission seen results from the interference of the radiation emitted all along the N periods. Constructive interference takes place at the 'resonant' wavelength such that the light moves exactly one period ahead of an electron while it crosses a single period of the undulator. This resonant wavelength also depends on the direction of observation defined by the angles θ (horizontal) and ψ (vertical). It is easily shown to be :

$$\lambda_r = \frac{\lambda_0}{2\gamma} \left(1 + \frac{K^2}{2} + \gamma^2 (\theta^2 + \psi^2) \right) \quad (4-3)$$

while the associated photon energy ε_r is :

$$\varepsilon_r [\text{keV}] = \frac{0.95 E^2 [\text{GeV}]}{\lambda_0 [\text{cm}] \left(1 + \frac{K^2}{2} + \gamma^2 (\theta^2 + \psi^2) \right)} \quad (4-4)$$

The emission presents a peak at this photon energy, its width being determined by the number of periods. In practical situations, the electron beam angular divergence spreads the resonant energy resulting in a broadening of the peak.

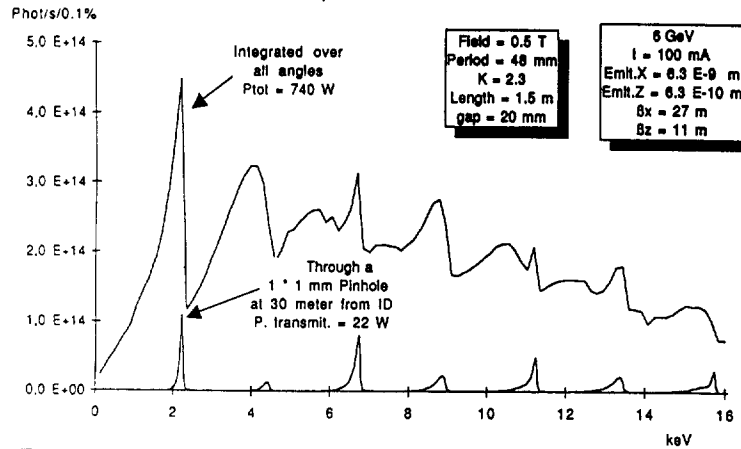


Fig. 3 Spectrum of an undulator installed at the ESRF

For intermediate K , significant emission occurs at wavelength harmonics of λ_r (higher order resonance). Such resonance occurs at a photon energy equal to $n\epsilon_r$ where n is an integer defining the harmonic number.

An undulator spectrum seen through a narrow pinhole presents a series of peaks as shown in Fig.3. The undulator is 1.5 m long, with 0.5 Tesla field and a 48 mm period ($K = 2.3$). The electron energy is 6 GeV, the current 100 mA. The narrow spectrum is seen through a square 1mm pinhole located 30 m away from the undulator. The shape of the peak is highly dependent on the angular spread of the electron beam (36 μ rad horizontal, 18 μ rad vertical FWHM).

As for the wiggler case, one defines the critical harmonic number n_c (median of the power spectrum) as:

$$n_c = 0.75 K (1+K^2/2) \quad (4-5)$$

Clearly the definition of n_c only make sense if $K > 1$.

For a large value of n_c the relative distance between the harmonics decreases and the spectra of the harmonics tends to overlap. In the limit of complete overlapping the final spectrum becomes similar to the one of a bending magnet or wiggler. For instance, wiggler radiation (as discussed above) can be seen as a particular case of undulator radiation in which a complete overlap of the harmonic spectra takes place. This last sentence expresses the expected continuity between undulator and wiggler radiation as one continuously changes K from a low to a high value.

Note that the photon energy defining the onset of overlapping strongly depends on many parameters such as electron beam divergences and sizes, and phase-space domain on which the spectrum is integrated. This is illustrated by Fig.3. The lower curve is the spectrum recorded on a narrow 1x1 mm pinhole located on the axis of a $K = 2$ undulator, it clearly presents individualised peaks at least up to the seventh. The upper curve is the flux recorded without a pinhole by integrating the radiation over the whole space. The lower the emittance of the beam, the sharper the peaks in Fig.3.

Note that any wiggler (defined as a high K ID) presents an undulator spectrum (with well defined peaks) in the low energy side of the spectrum. However, the power involved is usually negligible, and the fundamental of these peaks occurs at a very low energy (compared to the critical energy). This is easily seen from Eqs. (4-1) and (4-9). Similarly the very high energy side of the spectrum from an undulator (defined as a low K ID) can be just as smooth as a bending magnet spectrum.

Undulator radiation resulting from an interference process can be very intense in a small domain of the phase space where constructive interference occurs implying (in extreme cases) a spectral intensity proportionnal to N^2 rather than N as for a wiggler. To properly quantify this statement, one usually defines three representative quantities :

- Spectral flux [photons/second/0.1 % of bandwidth] for undulators, or in [photons/second/mrad/0.1 % of bandwidth] for wiggler and bending magnets
- Spectral brightness [photons/second/mrad²/0.1 % of bandwidth]
- Spectral brilliance [photons/second/mm²/mrad²/0.1 % of bandwidth]

The word spectral is often omitted. Note that each quantity results from a partial integration of the brilliance over the 4-dimensional transverse phase space. From the Liouville theorem the brilliance remains constant along the beamline if only drift and aberration free focusing elements are used. The relevant figure of merit can be either one of these three quantities (or an intermediate one) according to the experiment and the beamline design. Analytical expressions of such quantities have been derived for undulators and wigglers by various authors [9]. Essentially undulator peaks achieve the highest brilliance and brightness. Fluxes are quite similar for wiggler and undulator radiation. Figure 4 presents a comparison of the spectral brilliance which will be available from various representative ID at the ESRF.

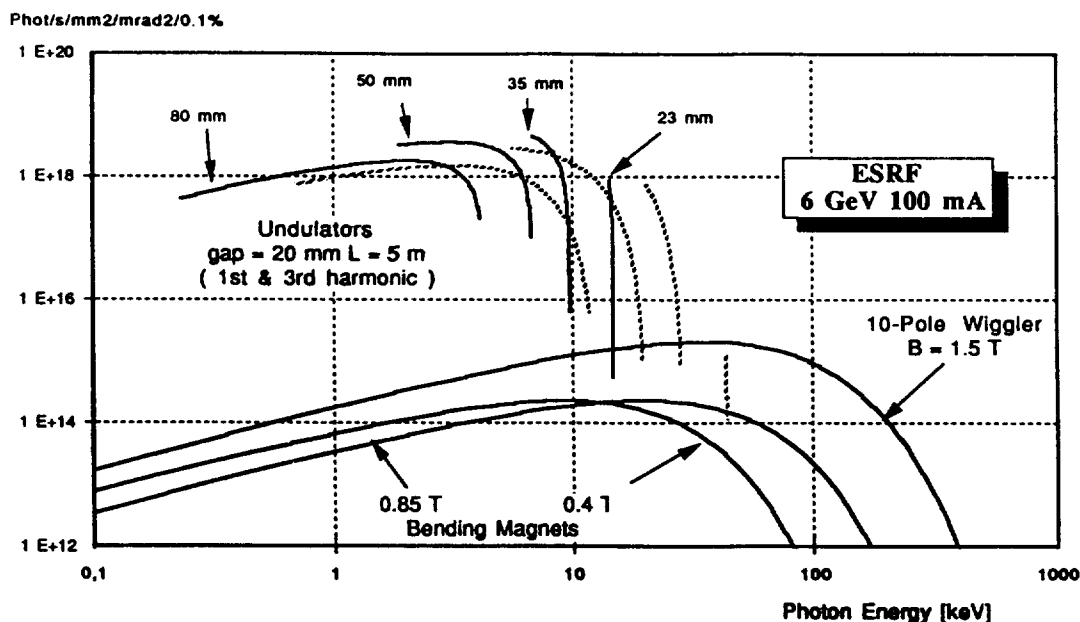


Fig. 4 Brilliance of various undulators and wigglers installed at the ESRF

When designing a beamline and its associated ID, one faces the problem of what value to choose for K . The answer depends in fact on only a few parameters : the electron energy, the minimum magnetic gap possible and the photon energy range to be spanned. In most experiments using a monochromator, one should always try to work in the undulator regime with the lowest possible harmonic number. However this is only possible in a restricted range of photon energies. The high boundary is determined by the minimum gap, the technology of construction of the ID and the electron energy. Any machine presents its own photon energy range on which high brightness and brilliance undulators can be used. Table 1 gives typical values for three machines of the third generation :

Table 1

Machine	Electron energy [GeV]	Main photon energy range for undulator radiation [keV]
SuperACO	0.8	0.01 to 0.2
ALS / ELETTRA / BESSY II	1.5	0.05 to 1
ESRF / APS	6	1 to 20

To design an experiment for a photon energy below this range, one faces a large fraction of unwanted hard radiation which heats the optical elements. To avoid this one can use an ID with an extremely low field and a few long periods (easy to build from a technological point of view) which gives poor brightness and brilliance as compared to an optimized ID on a lower energy machine. On the other hand, to use photon energies above this range requires a high order harmonic or a wiggler at the price of a reduced brightness and brilliance.

The total power (integrated over phase space and photon energy) generated by an insertion device is simply :

$$P \text{ [kW]} = 0.633 E^2 \text{ [GeV]} B^2 \text{ [T]} L \text{ [m]} I \text{ [Amp]} \quad (4-6)$$

where L is the length of the ID, and I is the stored current. The on-axis power density is [10] :

$$dP/d\theta d\psi \text{ [W/mrad}^2\text{]} \approx 10.8 B \text{ [T]} E^4 \text{ [GeV]} I \text{ [Amp]} N G(K) \quad (4-7)$$

with

$$G(K) = K \frac{K^6 + \frac{24}{7} K^4 + 4 K^2 + \frac{16}{7}}{(1 + K^2)^{\frac{7}{2}}} \quad (4-8)$$

Equations (4-7) and (4-8) express a linear increase of power and power density versus ID length and stored current. However, the electron energy dependence is strong and brings considerable heat load problems to high electron energy machines. Table 2 gives P and $dP/d\theta d\psi$ calculated for a similar simple ID (gap = 20 mm, $B = 0.5$ T, $\lambda_0 = 5$ cm, $L = 1.5$ m) installed on three machines operated at their nominal current:

Table 2

Machine	Electron energy [GeV]	Current [Amp]	Fundamental [keV]	Power [kW]	Power density [kW/mrad ²]
SuperACO	0.8	0.5	0.033	0.076	0.033
ALS / ELETTRA	1.5	0.4	0.1	0.21	0.6
ESRF	6	0.1	1.9	.85	21

Note that the radiation spot of such an undulator placed on the ESRF and observed from a 30 m distance presents a peak power density of 23 W/mm² (!). The focusing of such radiation would result in power densities more akin to a high power welding laser than a laboratory instrument. Very serious problems arise in the storage ring if the beam is deflected onto the vacuum chamber wall. A direct calculation from Eq. (4-6) taking a 5 m long 1.8 T wiggler (which from a technological point of view is not difficult) installed at the ESRF gives 37 kW of integrated power and 63 kW/mrad² power density. Such powers are, for the moment, higher than can be safely handled by front-end absorbers and beamline optical elements. One must keep in mind that, after monochromatisation, the useful beam is only in the milliwatt range and does not cause a significant heat load problem in the rest of the beamline. The key element is not only the ID but also the very first optical element (mirror or monochromator). One way to decrease the loading of that element while keeping a high spectral flux (brightness or brilliance) is to filter the undulator radiation with a narrow pinhole. Ultimately, the whole power will fall within the energy bandwidth of the monochromator which is not the case in present synchrotron sources. In other words, the improvement of the electron emittance not only results in a higher brilliance but also in the possibility of a better screening of the unwanted radiation, thus reducing heat load on the first optical element.

Radiation emitted on-axis is very highly linearly polarised in the horizontal plane.

The longitudinal coherence of the radiation is essentially determined by the spectral width which depends on the number of periods, electron angular spread and size, and on the volume of the 4-dimensional transverse phase space in which the radiation is collected. Using a very narrow pinhole, a small emittance electron beam and a well matched optical beam line, one approaches the limiting maximum coherence length of the nth harmonic :

$$l_c = nN\lambda_r$$

The transverse coherence highly depends on the emittance of the electron beam. Complete transverse coherence is approached if both emittances ϵ_x and ϵ_z are less than $\lambda/4\pi$

5. COMPUTATION OF THE SYNCHROTRON RADIATION

Let us now consider a population of N electrons in arbitrary motion and let $\vec{r}_j(t)$ and $\vec{\beta}_j(t)$ be the position and the velocity (normalized to the velocity of light) of the electron j at time t . Such a motion can be derived from the magnetic field configuration and the electrons' initial conditions. The number of photons \mathcal{F} generated in the solid angle $\Delta\Omega$ in the direction \vec{n} (real unitary vector) in the frequency range $\Delta\omega$ with the polarization defined by \vec{u} (complex unitary vector) is, at a sufficiently large distance from the electrons, given by [11, 12] :

$$\mathcal{F}(\omega, \vec{n}, \vec{u}) = \alpha \Delta\Omega \frac{\Delta\omega}{\omega} \left| \sum_{j=1}^N \vec{A}_j(\omega) \vec{u} \right|^2 = \alpha \Delta\Omega \frac{\Delta\omega}{\omega} \sum_{j=1}^N \sum_{k=1}^N \left(\vec{A}_j(\omega) \vec{u} \right) \left(\vec{A}_k^*(\omega) \vec{u} \right) \quad (5-1)$$

where α is the fine structure constant :

$$\alpha = \frac{e^2}{4\pi\epsilon_0 \hbar c} = \frac{1}{137} \quad (5-2)$$

and

$$\vec{A}_j(\omega) = \frac{\omega}{2\pi} \int_{-\infty}^{\infty} \vec{n} \times \left(\vec{n} \times \vec{\beta}_j \right) e^{i\omega \left(t - \frac{\vec{n} \cdot \vec{r}_j}{c} \right)} dt \quad (5-3)$$

$\vec{A}_j(\omega)$ is a complexe amplitude vector defining the amplitude of the wave (expressed in the frequency domain) generated by the electron j . The amplitude vector expressed in the time domain can be obtained from :

$$\vec{\tilde{A}}_j(t) = \frac{1}{\sqrt{2\pi}} \int_{-\infty}^{\infty} \vec{A}_j(\omega) e^{i\omega t} d\omega \quad (5-4)$$

Note that $\vec{A}_j(\omega)$ is always orthogonal to the direction of observation \vec{n} . Table 3 gives the expression of \vec{u} for various pure polarization states where \vec{x} and \vec{z} are respectively the horizontal and vertical unitary vectors. The convention used in the Table 3 is that a plane wave is horizontally polarized if the electric field is in the horizontal plane.

\vec{u}	Table 3 Polarization state	Photon flux
\vec{x}	Linear horizontal	\mathcal{F}_X
\vec{z}	Linear vertical	\mathcal{F}_Z
$(\vec{z} + \vec{x})/\sqrt{2}$	Linear at 45 degrees	\mathcal{F}_{45}
$(\vec{z} - \vec{x})/\sqrt{2}$	Linear at 135 degrees	\mathcal{F}_{135}
$(\vec{z} + i\vec{x})/\sqrt{2}$	Circular right	\mathcal{F}_R
$(\vec{z} - i\vec{x})/\sqrt{2}$	Circular left	\mathcal{F}_L

The number of photons originating from the electron bunch (defined by Eq. (5-1)) contains N^2 complexe terms. Usually, the distance between the electrons inside a bunch is random and as a consequence the non-diagonal terms in the double sum of (5-1) are randomly positive and negative but zero on average. Keeping only the diagonal terms, one rewrites (5-1) :

$$\mathcal{F}(\omega, \vec{n}, \vec{u}) = \alpha \Delta\Omega \frac{\Delta\omega}{\omega} \sum_{j=1}^N \left| \vec{A}_j(\omega) \vec{u} \right|^2 \quad (5-5)$$

or for a current I of electrons, neglecting the angular and energy spreads:

$$\frac{d\mathcal{F}(\omega, \vec{n}, \vec{u})}{dt} = \alpha \Delta\Omega \frac{\Delta\omega}{\omega} \frac{I}{e} \left| \vec{A}(\omega) \vec{u} \right|^2 \quad (5-6)$$

At this point, it is important to notice that the simplification from (5-1) to (5-5) is only valid if one wants to calculate the "incoherent" photon flux. If the electron motion is perturbed by an external plane wave field (Laser field for example), the field generated by a single electron is the sum of the unperturbed one, that induced by the perturbing plane wave, and the laser field itself. Then the double sum (5-1) presents a large number of terms. Some terms contribute proportionally to N^2 , so determining the generation of coherent synchrotron radiation which is observed under the excitation by an external laser. Some other terms are proportional to the external field power, it defines an amplification or absorption and being the basis of the FEL. In the terminology used for FEL's, the radiation given by (5-5) is the spontaneous emission. One way to understand the interest of FEL's is their enhancement of the spontaneous emission towards a higher power, spectral flux brightness or brilliance.

In the following, I shall assume that a bunch of ultra-relativistic electrons propagates in a direction s with a very small angular spread. Let x and z be two orthogonal directions such that x, z, s define an orthogonal set of coordinates. x, z and s will also be called the horizontal, vertical and longitudinal coordinates. The Lorentz force equation :

$$\frac{d\vec{\beta}}{dt} = -\frac{e}{\gamma m} \vec{\beta} \times \vec{B} \quad (5-7)$$

with

$$\gamma = \frac{1}{\sqrt{1-\vec{\beta}^2}} \quad (5-8)$$

can be rewritten :

$$\frac{d}{ds} \begin{pmatrix} \beta_x \\ \beta_z \end{pmatrix} = \frac{e}{\gamma m c} \begin{pmatrix} B_z(s) \\ -B_x(s) \end{pmatrix} \quad (5-9)$$

$$\beta_s = 1 - \frac{1}{2\gamma^2} - \frac{\beta_x^2}{2} - \frac{\beta_z^2}{2} \quad (5-10)$$

where γ is a constant of the motion.

Let's define the angle of observation $\theta_x \ll 1$ and $\theta_z \ll 1$ such that

$$\vec{n} = \left(\theta_x, \theta_z, 1 - \frac{\theta_x^2}{2} - \frac{\theta_z^2}{2} \right) \quad (5-11)$$

Then (5-3) can be rewritten :

$$\begin{pmatrix} A_x \\ A_z \end{pmatrix} = \frac{1}{\lambda} \int_{-\infty}^{+\infty} \begin{pmatrix} \theta_x - \beta_x \\ \theta_z - \beta_z \end{pmatrix} e^{i\Phi} ds \quad (5-12)$$

with

$$\frac{d\Phi}{ds} = \frac{\pi}{\lambda} \left(\frac{1}{\gamma^2} + (\theta_x - \beta_x)^2 + (\theta_z - \beta_z)^2 \right) \quad (5-13)$$

where λ is the wavelength of the wave ($\lambda = 2\pi c/\omega$).

Equations (5-9) to (5-13) together with (5-6) are the basis of any computation of synchrotron radiation characteristics. The radiation from bending magnets, conventional undulators and wigglers, helical undulators, assymetric wigglers... can be described by using the proper field geometry.

Using the variable μ defined as :

$$\begin{pmatrix} \mu_x \\ \mu_z \end{pmatrix} = \gamma \begin{pmatrix} \beta_x - \theta_x \\ \beta_z - \theta_z \end{pmatrix} \quad (5-14)$$

one can rewrite (5-9) and (5-12) as :

$$\frac{d}{d\varphi} \begin{pmatrix} \mu_x \\ \mu_z \end{pmatrix} = \frac{2}{1+\mu} \frac{c}{mc} \begin{pmatrix} B_z(s) \\ -B_x(s) \end{pmatrix} \quad (5-15)$$

$$\frac{ds}{d\varphi} = \frac{2}{1+\mu} \quad (5-16)$$

$$\begin{pmatrix} A_x \\ A_z \end{pmatrix} = \frac{2}{\lambda \gamma} \int_{-\infty}^{+\infty} \frac{1}{1+\mu} \begin{pmatrix} \mu_x \\ \mu_z \end{pmatrix} e^{i\left(\frac{2\pi\varphi}{\lambda\gamma^2}\right)} d\varphi \quad (5-17)$$

A very efficient computation of $A_x(\omega)$ and $A_z(\omega)$ is possible through the use of a Runge Kutta integration and fast Fourier transform. By replacing $A_x(\omega)$ and $A_z(\omega)$ in Eq. (5-5), one computes the spectral flux and spectral brightness at any polarization state.

When dealing with polarization, one usually defines the following three polarization rates :

$$\begin{aligned}
 P_1 &= \frac{F_x - F_z}{F_x + F_z} && \text{Normal linear polarization rate} \\
 P_2 &= \frac{F_{45} - F_{135}}{F_{45} + F_{135}} && \text{Linear polarization rate at 45 degrees} \\
 P_3 &= \frac{F_R - F_L}{F_R + F_L} && \text{Circular polarization rate}
 \end{aligned}$$

where $F_x, F_z, F_{45}, F_{135}, F_R, F_L$ are defined in Table 3. One can show that the polarization rates satisfy :

$$P_1^2 + P_2^2 + P_3^2 \leq 1 \quad (5-18)$$

For a single electron, integrating the photon flux over an infinitely small solid angle, one obtains equality in Eq. (5-18). One can show from Eq. (5-5) that the inequality sign is generated by the summation over the electron population and the integration over a finite solid angle and frequency spectrum. The occurrence of strict inequality in Eq. (5-18) can be interpreted as the presence of unpolarized radiation (or natural radiation). Very generally, the polarization rates are highly dependent on the field configuration, the detector size and selectivity, and electron beam energy spread, angular divergence and sizes.

The three components P_1, P_2 and P_3 can be interpreted as the three components of the Stokes-Poincare vector \vec{P} . A more modern analysis can be made by mean of the 2*2 density matrix M :

$$M = \frac{1}{2} (1 + \vec{P} \cdot \vec{\sigma})$$

where $\vec{\sigma}$ are the three 2x2 Pauli matrices.

BIBLIOGRAPHY

- J.D. Jackson, "Classical Electrodynamics", chapter : "Radiation by Moving Charges", John Wiley (New York).
- H. Winick, G. Brown, K. Halbach, J. Harris, "Wiggler and Undulator magnets", Physics today, May 1981
- G. Brown, K. Halbach, J. Harris, H. Winick, " Wiggler and Undulator magnets - A review", Nucl. Instr. and Methods, 208, p65-77
- Proceedings of the International Conference on Insertion Devices for Synchrotron Sources. SPIE, Vol. 582 - 1985
- S. Krinsky, M.L. Perlman, R.E. Watson, "Characteristics of Synchrotron Radiation and its Sources", Handbook on Synchrotron Radiation, Vol 1a, North Holland 1983.
- K.J. Kim, "Characteristics of Synchrotron Radiation", Proceedings of the US Particle Accelerator School, 1987.

REFERENCES

- [1] H. Motz, W. Thon, R.N. Whitehurst, J. Appl. Phys. 24, p826 (1953).
- [2] L.R. Elias, W.M. Fairbank, J.M.J. Madey, H.A. Schwettman, T.I. Smith, Phys. Rev Lett. 36, p717 (1976).
- [3] K.W. Robinson, Phys. Rev. 3, p373 (1958).
- [4] R. H Helm, M.J. Lee, P. L. Morton, M. Sands, IEEE Trans. Nucl. Sci. Ns-20, 900 (1973).
- [5] M. Sands, The Physics of Electron Storage Rings. An Introduction, Proc. of the Intern. School Enrico Fermi, p257 (1971).
- [6] A. Blondel, J. M. Jowett, LEP Note 606.
- [7] Y. Baconnier, et al., Nucl. Instr. and Meth., A234, p244-252 (1985).
- [8] J. M. Jowett, T.M. Taylor, IEEE Trans. Nucl. Sci. 30, p2583 (1983).
- [9] S. Krinsky, IEEE Trans. Nucl. Sci., Ns-30, p3078, (1983)
R. Coisson, R.P. Walker, SPIE vol. 582, p24-29 (1985).
K.J. Kim, SPIE vol. 582, p2-9 (1985).
K.J Kim, X-ray Data Booklet, section 4, PUB-490 Lawrence Berkeley Lab
- [10] K.J. Kim, Nucl. Instr. and Methods, A246, p67-70 (1986).
- [11] J. Schwinger, Phys. Rev. 75, p1912 (1949).
- [12] J. D. Jackson, "Classical Electrodynamics", chapter 14, John Wiley (NY).

